

Frustrated magnetization in Co nanowires: Competition between crystal anisotropy and demagnetization energy

Gerd Bergmann,* Jia G. Lu, Yaqi Tao, and Richard S. Thompson

Department of Physics, University of Southern California, Los Angeles, California 90089-0484, USA
(Received 23 August 2007; revised manuscript received 26 October 2007; published 13 February 2008)

Cobalt nanowires with a diameter in the range between 50 and 100 nm can be prepared as single-crystal wires with the easy axis (the c axis) perpendicular to the wire axis. The competition between the crystal anisotropy and demagnetization energy frustrates the magnetization direction. Using a trial function, we find that the energy is lowered when the magnetization modulates its orientation within the plane spanned by the wire axis and the easy axis. The angle relative to the wire axis varies as $\theta = \theta_0 \cos(kz)$. We calculate the energy of this modulated magnetization in the thin-wire limit where the magnetization is constant within a cross section. The optimal period and amplitude of the modulation are numerically determined for the bulk parameters of Co. The period is about three times the wire radius and the amplitude about 1 rad.

DOI: 10.1103/PhysRevB.77.054415

PACS number(s): 76.50.+g, 75.25.+z, 75.30.Ds, 75.30.Gw

In recent years, a great interest has developed in dynamic magnetic torque experiments on magnetic nanostructures (see, for example, Ref. 1). These experiments explore the possibility of rotating the orientation of the magnetization with a current pulse. This could be an important tool in spintronics. Complementary to the dynamic experiments, we want to explore the static properties of magnetic nanostructures, particularly cobalt nanowires (NWs). We believe that a detailed knowledge of the static magnetic properties will have important consequences in their dynamic behavior.

A number of experimental groups²⁻⁹ have prepared Co NWs with diameters in the range of 30 nm to several hundreds of nanometers. Similar Co NWs with a diameter of 80 nm were recently fabricated at the University of Southern California.¹⁰ In some of the experiments, the magnetic structure of the NWs was investigated with a magnetic force microscope (MFM).^{2,8,7,10} The MFM scan showed spatial oscillations of the magnetic field along the length of the wire, which are sometimes quasiperiodic. Thiaville *et al.*¹¹ concluded that in their experiments the period is in agreement with a “head-to-head” magnetization, a 180° Bloch wall.

Henry *et al.*⁷ observed by means of dark field transmission electron microscopy images that the Co NWs have the bulk hexagonal structure. For wire diameters $2R < 50$ nm, the easy c axis lies parallel to the wire axis, while for NWs with diameters of $2R > 50$ nm, the easy c axis is perpendicular to the NW axis. In the following, we discuss the latter case, NWs with a diameter of $2R > 50$ nm. Below, we choose a radius of $R = 40$ nm for quantitative calculations. We denote the wire axis as the z direction and the easy axis as the x direction of our coordinate system.

When the axis of the Co NW and the easy axis lie perpendicular to each other, then the magnetization is frustrated. The shape or demagnetization anisotropy prefers to align the magnetization in the z direction, parallel to the wire axis. However, the crystal anisotropy definitely favors the x direction. Moreover, this crystal anisotropy is very large in the uniaxial Co wire.

The shape or demagnetization anisotropy energy density (ED) is due to the demagnetization field and for constant magnetization density is given by

$$u_d = \frac{\mu_0}{2} \mathbf{N} \mathbf{M} \mathbf{M} = -\frac{\mu_0}{2} \mathbf{H} \cdot \mathbf{M},$$

where \mathbf{N} is the 3×3 demagnetization matrix, \mathbf{H} is the demagnetization field, i.e., the magnetic field in the absence of an external magnetic field, and \mathbf{M} the magnetization. We introduce θ as the angle between the z or wire axis and the magnetization \mathbf{M} . (Within this paper, the magnetization will always lie in the x - z plane.) Then, one has a demagnetization factor of $N_{xx} = \frac{1}{2}$ for $\theta = \pi/2$ (perpendicular to the wire) and $N_{zz} = 0$ for $\theta = 0$ (parallel to the wire axis). For a constant magnetization $\mathbf{M} = M_0(\sin \theta, 0, \cos \theta)$ at the angle θ , the demagnetization energy density is

$$u_d = \frac{1}{2} \sin^2 \theta \left(\frac{\mu_0}{2} M_0^2 \right).$$

We take from O’Handley¹² the reference value for the magnetic ED of Co $u_{00} = \frac{\mu_0}{2} M_0^2 = 12 \times 10^5$ J/m³. The value of u_d/u_{00} is 0 for \mathbf{M} parallel to the wire axis and 1/2 for \mathbf{M} parallel to the easy axis.

The energy density of the crystal anisotropy is generally given in terms of the angle between the easy axis and the magnetization. In our geometry, this angle is equal to $(\frac{\pi}{2} - \theta)$. The crystal anisotropy ED is, in terms of this angle θ ,

$$u_{ca} = k_1 \cos^2 \theta + k_2 \cos^4 \theta.$$

The crystal anisotropy constant k_1 is given in the literature as $k_1 = 4.1 \times 10^5$ J/m³.¹² For the constant k_2 , one finds different values in the literature, for example, $k_2 = 1.5 \times 10^5$ J/m³ (Ref. 12) and $k_2 = 1.0 \times 10^5$ J/m³.¹³ The resulting crystal anisotropy ED u_{ca}/u_{00} is 0.47 (0.425 for $k_2 = 1.0 \times 10^5$ J/m³) along the wire axis and 0 parallel to the easy axis.

Obviously, the competition between the crystal anisotropy and demagnetization is a close call. The system will try to reduce its energy as much as possible by the crystal anisotropy without paying too much energy to the demagnetization energy. The case of competing lattice anisotropy and dipole coupling is also present in thin films with perpendicular anisotropy (see, for example, Refs. 14 and 15).

One way to reduce the demagnetization energy is to

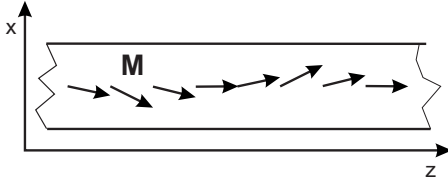


FIG. 1. Nanowire with magnetization modulation along the z axis.

modulate the magnetization direction in the x - z plane so that the angle θ between \mathbf{M} and \hat{z} oscillates as $\theta = \theta_0 \cos(kz)$. (There is no oscillation in time but only in space in contrast to spin waves in NWs, which have been treated by Arias and Mills¹⁶). While for a constant magnetization in the x direction the field \mathbf{H} falls off as $1/\rho^2$ with the distance ρ from the wire axis, a modulated magnetization with a period λ will cancel the field for distances ρ , which are larger than λ . This reduces the demagnetization ED. In this paper, we investigate the effect of such a modulation on the ED for very thin wires. When the diameter of a ferromagnetic wire is smaller than the exchange length, the direction of the magnetization is constant within a cross section of the wire. We denote this case as the thin-wire limit.

The modulation $\theta = \theta_0 \cos(kz)$ yields the magnetization

$$\mathbf{M} = M_0 [\sin(\theta_0 \cos kz), 0, \cos(\theta_0 \cos kz)].$$

In Fig. 1, the orientation of the magnetization is shown as a function of z . We keep the absolute value of $|\mathbf{M}| = M_0$ constant.

The magnetization components M_x and M_z can be expressed as two Fourier series,

$$M_x(z) = M_0 \sum_{\nu=0}^{\infty} c_{2\nu+1} \cos[(2\nu+1)kz],$$

$$M_z(z) = M_0 \sum_{\nu=1}^{\infty} c_{2\nu} \cos(2\nu kz).$$

The coefficients $c_{2\nu+1}, c_{2\nu}$ can be easily obtained from a Fourier expansion of \mathbf{M} . The lowest coefficients are $c_0(\theta_0) = (1 - \frac{1}{4}\theta_0^2 + \frac{1}{64}\theta_0^4 - \dots)$, $c_1(\theta_0) = (\theta_0 - \frac{1}{8}\theta_0^3 + \frac{1}{192}\theta_0^5 - \dots)$, etc. We include terms up to the order of θ_0^8 .

In the next step, we calculate the demagnetization field \mathbf{H} for a magnetization $M_x = M_{x0} \cos(qz)$. Setting $q = (2\nu+1)k$ and $M_{x0} = M_0 c_{2\nu+1}$ afterward, the results can be used for each Fourier component.

The magnetic flux \mathbf{B} inside and outside of the sample is given by $\mathbf{B} = \mu_0(\mathbf{H} + \mathbf{M})$. Since there are no external currents in our problem, the curl of the magnetic field vanishes, $\nabla \times \mathbf{H} = 0$. Therefore, the magnetic field can be expressed as the gradient of a magnetic potential $\mathbf{H} = -\nabla \phi$ (in full analogy with the electrostatic case). This magnetic potential is due to the magnetic surface charges, which are generated by the modulation of the magnetization. This surface charge yields a discontinuity of the magnetic field component H_{\perp} perpendicular to the surface of the wire.

Taking the divergence of the magnetic flux (which vanishes) yields

$$0 = \nabla \cdot \mathbf{B} = \mu_0(\nabla \cdot \mathbf{H} + \nabla \cdot \mathbf{M}),$$

and replacing the field by the potential yields

$$\Delta \phi = \nabla \cdot \mathbf{M}.$$

For M_x , the divergence of \mathbf{M} is zero.

We use cylindrical coordinates (ρ, φ, z) and take the φ dependence as $\cos \varphi$. Then, the solutions of the Laplace equation are

$$\phi = \begin{cases} C^{in} I_1(q\rho) \cos \varphi \cos qz, & \rho < R \\ C^{out} K_1(q\rho) \cos \varphi \cos qz, & \rho > R \end{cases}.$$

where $I_1(s)$ and $K_1(s)$ are modified Bessel functions. The coefficients C^{in} and C^{out} are obtained by using the boundary conditions at $\rho = R$. The components B_{ρ} and H_{φ} have to be continuous. This yields $C^{in} = RM_{x0} K_1(qR)$ and $C^{out} = RM_{x0} I_1(qR)$. [In determining the coefficients, one obtains the Wronski determinant $W = [I_1(qR)K_1'(qR) - I_1'(qR)K_1(qR)]$ as a denominator, which has the value $W = -1/(qR)$].

From the magnetic potential, one obtains the components of the magnetic field \mathbf{H} . The x component of \mathbf{H} inside the wire is

$$H_x(\rho < R) = -qR K_1(qR) \left[I_1'(q\rho) \cos^2 \varphi + \frac{1}{q\rho} I_1(q\rho) \sin^2 \varphi \right] M_{0x} \cos(qz).$$

The local demagnetization ED is $-(\mu_0/2)H_x M_x$. We average over a period in the z direction and the cross section πR^2 and obtain for an individual Fourier component the demagnetization ED,

$$\left(\frac{\mu_0}{2} M_{x0}^2 \right) \frac{1}{2} K_1(qR) I_1(qR).$$

For each $q = (2\nu+1)k$, the demagnetization field \mathbf{H} interacts only with the magnetization \mathbf{M} of the same q (after averaging). Then, the total contribution of all components of M_x is just the sum of the individual contributions. In the following, we normalize all EDs by dividing by the value $u_{00} = \frac{\mu_0}{2} M_0^2$. Then, the normalized ED is

$$u_{00} = \sum_{\nu=0}^n [c_{2\nu+1}(\theta)]^2 \frac{1}{2} K_1[(2\nu+1)s] I_1[(2\nu+1)s],$$

where $s = kR$. In the numerical evaluation we include three terms (the third hardly contributes).

The Fourier components $M_z = M_{z0} \cos qz$ for the z component of the magnetization are calculated quite analogously. The main difference is that the magnetic field \mathbf{H} and, therefore, the magnetic potential are independent of φ . Therefore, ϕ is given by the modified Bessel functions $I_0(q\rho)$ and $K_0(q\rho)$ of order zero. Furthermore, $\Delta \phi$ does not vanish but is given by

TABLE I. For two values of k_2 and a_{ex} , the coordinates and the value of the (normalized) energy density (ED) in the s - θ_0 plane are collected in columns 3, 4, and 5. Columns 6 and 7 give the ED for a constant magnetization parallel to the z and the x axis.

k_2/u_{00}	a_{ex}/u_{00} (10^{-2})	s_{\min}	θ_{\min}	u_{\min}/u_{00}	$u[\mathbf{M}\parallel\hat{z}]$	$u[\mathbf{M}\parallel\hat{x}]$
0	0.68	2.3	0.7	0.333 88	0.34	0.5
0	1.36	1.75	0.3	0.341 37	0.34	0.5
0.083	0.68	2.1	1.0	0.378 83	0.425	0.5
0.083	1.36	1.6	0.8	0.396 9	0.425	0.5
0.125	0.68	2.1	1.0	0.397 04	0.47	0.5
0.125	1.36	1.5	0.9	0.417 71	0.47	0.5

$$\Delta\phi = \frac{dM_z}{dz} = -M_{z0}q \sin(qz) \neq 0.$$

The solution is found in complete analogy to the M_x component and is given by

$$\phi(\rho, z) = RM_{z0} \sin(qz) \left\{ \begin{array}{l} \left[\frac{1}{qR} + K'_0(qR)I_0(q\rho) \right], \quad \rho < R \\ I'_0(qR)K_0(q\rho), \quad \rho > R \end{array} \right\}.$$

The magnetic field component H_z inside the wire is

$$H_z(\rho < R) = -[qRK'_0(qR)I_0(q\rho) + 1]M_{z0} \cos qz.$$

In the evaluation of the demagnetization ED, we use the identities $tI_0(t) = d[tI_1(t)]/dt$, $K'_0(t) = -K_1(t)$, and $I'_0(t) = I_1(t)$. The averaged demagnetization ED becomes $(\frac{\mu_0}{2}M_{z0}^2) [\frac{1}{2} - K_1(qR)I_1(qR)]$. The contribution of all Fourier components of M_z is

$$\frac{u_z(s, \theta_0)}{u_{00}} = \sum_{\nu=1}^{\infty} [c_{2\nu}(\theta)]^2 \left(\frac{1}{2} - K_1(2\nu s)I_1(2\nu s) \right).$$

Again, we include the first three terms in the numerical evaluation.

Next, we consider the crystal anisotropy ED. The average of the term $k_1 \cos^2 \theta$ yields

$$\frac{u_{ca}^{(1)}(\theta_0)}{u_{00}} = \frac{1}{u_{00}} \frac{1}{2\pi} \int_0^{2\pi} k_1 \cos^2[\theta_0 \cos(s)] ds = 0.34 \times a_1(\theta_0),$$

where $a_1(\theta_0) = 1 - \frac{1}{2}\theta_0^2 + \frac{1}{8}\theta_0^4 - \dots$. The average of the term $k_2 \cos^4 \theta$ yields

$$\frac{u_{ca}^{(2)}}{u_{00}} = 8.3 \times 10^{-2} \times a_2(\theta_0)$$

for $k_2 = 1.0 \times 10^5 \text{ J/m}^3$ with $a_2(\theta_0) = 1 - \theta_0^2 + \frac{5}{8}\theta_0^4 - \dots$. In both cases, we include terms up to the order of θ_0^{18} .

Finally, we have to include the exchange stiffness of the Co wire. While a modulation of the magnetization can reduce the demagnetization and the crystal anisotropy energy, it will cost energy because of the bending of the magnetization. The increase in the ED can be expressed in terms of the exchange stiffness constant D_{ex} ,

$$u_{ex} = \frac{1}{4g\mu_B} \frac{M_0}{\theta_0^2} D_{ex} k^2.$$

From Brown's equations,¹⁷ the boundary condition on the angle θ is that its normal derivative vanishes at the wire surface. The nonzero eigenvalues of the transverse component of k are quantized proportional to $1/R$. In the thin-wire limit, such contributions to u_{ex} can be neglected, which enforces a constant \mathbf{M} within the wire cross section. u_{ex} also suppresses higher Fourier components along the wire.

Liu *et al.*¹⁸ determined the exchange stiffness D_{ex} experimentally from the spin-wave spectrum in hexagonal Co. They also performed a theoretical calculation. From the experiment, they obtained $D_{ex} = 435 \text{ meV} \times A^2 = 6.96 \times 10^{-40} \text{ J m}^2$. Their theoretical result yielded twice this value. Using the experimental value and a radius of $R = 40 \text{ nm}$, we obtain $u_{ex} = 8125 \times (kR)^2 \theta_0^2 \text{ J m}^{-3}$. The normalized exchange stiffness ED is then

$$\frac{u_{ex}}{u_{00}} = a_{ex} s^2 \theta_0^2, \quad a_{ex} = 0.68 \times 10^{-2}.$$

This exchange ED is very small compared with the demagnetization and the crystal anisotropy EDs, which are of the order of 1.

Finally, we add all terms and calculate the total ED as a function of $s = kR$ and θ_0 and determine the minimum of this energy,

$$u_i(s, \theta) = \frac{1}{u_{00}} [u_x(s, \theta_0) + u_z(s, \theta_0) + u_{ca}(\theta_0) + u_{ex}(s, \theta_0)].$$

We perform the calculation for different choices of the parameter k_2 and determine the position of the minimum of the ED in the s - θ_0 plane. To investigate the effect of the exchange ED, we also perform a calculation with twice the experimental value for a_{ex} . In Table I, the numerical results for different parameter choices are collected.

For $k_2/u_{00} = 0.083$ and $a_{ex} = 0.68 \times 10^{-2}$, we find the minimum at $(s, \theta_0) = (2.1, 1.0)$. In Figs. 2(a) and 2(b), the dependence of u_i/u_{00} is plotted for these parameters. The figures show two orthogonal traces through the energy minimum (a) along the $s = kR$ direction and (b) along the θ_0 direction.

For $\theta_0 = 1.0$, we can draw the two components $M_x = M_0 \sin(\theta_0 \cos kz)$ and $M_z = M_0 \cos(\theta_0 \cos kz)$ as a function

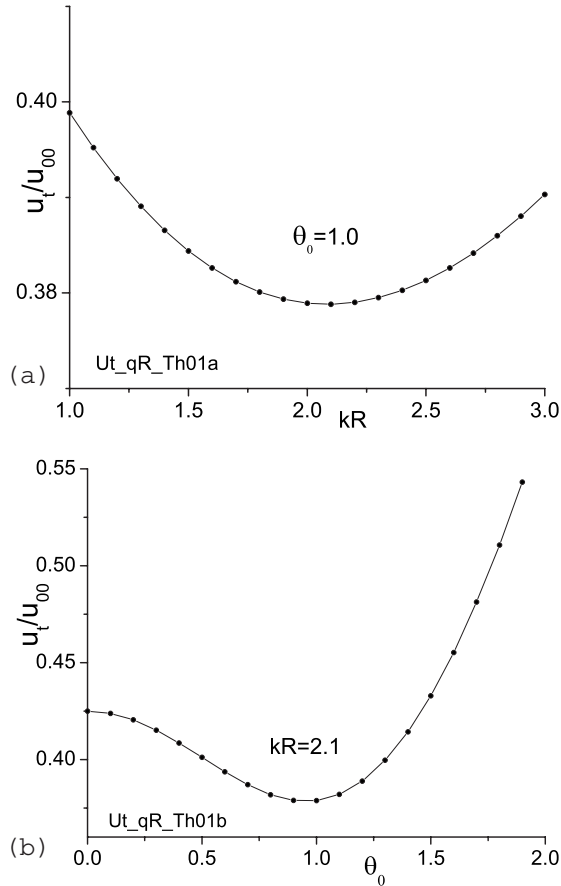


FIG. 2. [(a) and (b)] The ED as a function of $s=kR$ (3a) and θ_0 (3b) through the minimum for the parameters $k_2/u_{00}=0.083$ and $a_{ex}/u_{00}=0.68 \times 10^{-2}$.

of z along the wire. This is shown in Fig. 3. With $\theta = 1.0 \cos(kz)$, the amplitude of the angle is less than $\pi/2$. Therefore, the z component never reverses direction. At $kz = \nu\pi$, the x component takes the value $M_x = M_0 \sin(\pm \theta_0) = \pm 0.84M_0$ and reaches almost the saturation magnetization.

There has been the suggestion¹¹ that the magnetization varies head to head with a 180° Bloch wall. Therefore, we

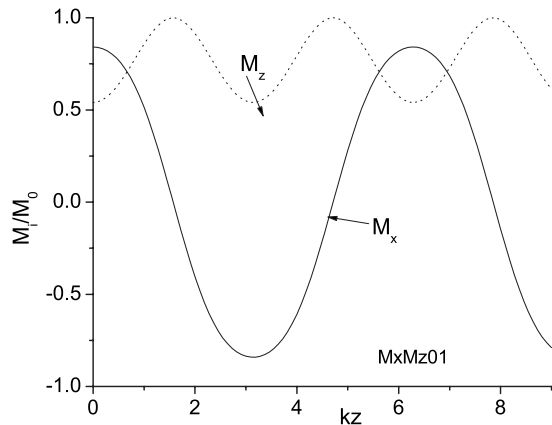


FIG. 3. The x and the z component of the magnetization as a function of position $s=kz$.

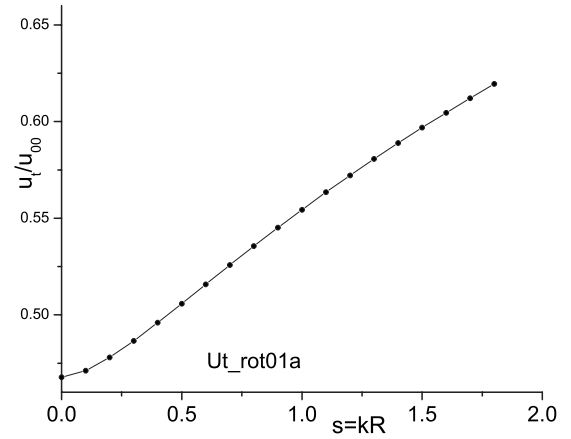


FIG. 4. The total energy density for a spatially rotating magnetization as a function of $s=kR$.

calculate for a comparison the ED when the magnetization angle rotates in the x - z plane as $\theta=kz$. This yields

$$\mathbf{M} = M_0[\sin(kz), 0, \cos(kz)].$$

In this case, we have only one Fourier component in x and z directions with the same wave number k . The demagnetization ED follows from the above calculation. (There is no cross term between the x and z parts of the demagnetization ED since their φ components are orthogonal.) The k_1 part of the crystal anisotropy ED has the weight $1/2$, and the k_2 has a weight of $3/8$. The exchange stiffness ED is just $u_{ex}/u_{00} = 0.68 \times 10^{-2} s^2$. Figure 4 shows the dependence of the total ED u_t/u_{00} as a function of $s=kR$. The total ED has its smallest value of $u_t/u_{00}=0.4677$ at $k=0$. Therefore, this behavior of the magnetization is energetically unfavorable.

Finally, we want to discuss the physics of the solution and compare it with the experiment. The physical interpretation of our result is the following: The form of the anisotropy energy is fixed. If there is no component of the magnetization in the x direction, then one loses the anisotropy energy. However, one can modify the demagnetization energy. In order to reduce the demagnetization energy, the magnetization does not have to point along the z axis. It is sufficient that it alternates its orientation along the x axis. Our calculation shows that the magnetic energy is thereby reduced. The shorter the period of the alternating magnetization, the smaller is the demagnetization energy. However, the period is limited by the exchange energy. The latter does not like a strong gradient of the angle θ of the magnetization. As a consequence, the angle does not alternate between $\pi/2$ and $-\pi/2$ but only between $+\theta_0$ and $-\theta_0$. Therefore, the overall magnetization has always a component in one direction of the nanowire axis. It never reverses its component parallel to the nanowire. This means that one expects always opposite poles at the two ends of the nanowire. (A fully rotating magnetization would yield an equal chance that the ends have the same or an opposite magnetic pole.) The period of the modulation is essentially determined by the exchange strength and is of the order of $3R$.

In the real world, the modulation of the magnetization has to overcome a serious obstacle, the pinning forces in the wire. The coercitive force is a manifestation of such pinning forces. However, there are a number of MFM images that show a quasiperiod modulation of the magnetic field along the Co NW, and they always show that the ends of the nanowire have opposite magnetic poles. In Ref. 7, Fig. 12, two MFM images of a Co NW, which is touched by a short NW, are shown. The images appear to show a periodic sequence of light and dark spots (the densimeter trace along the NW

does not resolve the fine structure). In Ref. 8, the MFM image of a Co NW with $2R=35$ nm shows a quasiperiodic field. However, the ratio of period to radius is not easily extracted from these images. Particularly good examples are the experiments by Belliard *et al.*² with [Co/Cu] NWs. For example, MFM images of a multiwire with (170 nm Co/10 nm Cu) appear to show opposite magnetizations for neighboring segments. We expect that the demagnetization ED causes an antiferromagnetic coupling between neighboring Co segments.

*bergmann@usc.edu

- ¹I. N. Krivorotov, N. C. Emley, J. C. Sankey, S. I. Kiselev, D. C. Ralph, and R. A. Buhrman, *Science* **307**, 228 (2005).
- ²L. Belliard, J. Miltat, A. Thiaville, S. Dubois, J. L. Duvail, and L. Piraux, *J. Magn. Magn. Mater.* **190**, 1 (1998).
- ³J. M. Garcia, A. Asenjo, J. Velazquez, D. Garca, M. Vazquez, P. Aranda, and E. Ruiz-Hitzky, *J. Appl. Phys.* **85**, 5480,(1999).
- ⁴J. E. Wegrowe, D. Kelly, A. Franck, S. E. Gilbert, and J. P. Ansermet, *Phys. Rev. Lett.* **82**, 3681 (1999).
- ⁵J. M. Garcia, A. Asenjo, M. Vazquez, P. Aranda, and E. Ruiz-Hitzky, *IEEE Trans. Magn.* **36**, 2981 (2000).
- ⁶T. Thurn-Albrecht, J. Schotter, G. A. Kästle, N. Emley, T. Shibauchi, L. Krusin-Elbaum, K. Guarini, C. T. Black, M. T. Tuominen, and T. P. Russell, *Science* **290**, 2126 (2000).
- ⁷Y. Henry, K. Ounadjela, L. Piraux, S. Dubois, J. M. George, and J. L. Duvail, *Eur. Phys. J. B* **20**, 35 (2001).
- ⁸J. M. Garcia, A. Thiaville, and J. Miltat, *J. Magn. Magn. Mater.* **249**, 163 (2002).
- ⁹H. Zeng, R. Skomski, L. Menon, Y. Liu, S. Bandyopadhyay, and D. J. Sellmyer, *Phys. Rev. B* **65**, 134426 (2002).
- ¹⁰Z. Liu, C. C. Chang, P. Chang, E. Galaktionov, and J. G. Lu (unpublished).
- ¹¹A. Thiaville, J. M. Garcia, and J. Miltat, *J. Magn. Magn. Mater.* **242**, 1061 (2002).
- ¹²R. C. O'Handley, *Modern Magnetic Materials: Principles and Applications* (Wiley, New York, 2000).
- ¹³D. Craik, *Magnetism Principles and Applications* (Wiley, New York, 1995).
- ¹⁴Y. Yafet and E. M. Gyorgy, *Phys. Rev. B* **38**, 9145 (1988).
- ¹⁵A. Hubert, and R. Schaefer, *Magnetic Domains: The Analysis of Magnetic Microstructures* (Springer, Berlin, 1999).
- ¹⁶R. Arias and D. L. Mills, *Phys. Rev. B* **63**, 134439 (2001).
- ¹⁷W. F. Brown, *Phys. Rev.* **58**, 736 (1940).
- ¹⁸X. Liu, M. M. Steiner, R. Sooryakumar, G. A. Prinz, R. F. C. Farrow, and G. Harp, *Phys. Rev. B* **53**, 12166 (1996).